Heterogeneous & Homogeneous & Bio- & Nano-
CHEMCATCHEM
CATALYSIS

Accepted Article

Title: Highly Dispersed Mo2C Anchored on N,P-codoped Graphene as Efficient Electrocatalyst for Hydrogen Evolution Reaction

Authors: Yang Wang, Shengdong Zhu, Noritatsu Tsubaki, and Mingbo Wu

To be cited as: *ChemCatChem* 10.1002/cctc.201800025

Link to VoR: http://dx.doi.org/10.1002/cctc.201800025

A Journal of
ChemPubSoc Europe

WILEY-VCH

www.chemcatchem.org

Highly Dispersed Mo_2C Anchored on N,P-codoped Graphene as Efficient Electrocatalyst for Hydrogen Evolution Reaction

Yang Wang,[a, b] Shengdong Zhu,[a] Noritatsu Tsubaki,*[b] and Mingbo Wu*[a]

Abstract: Uniformly dispersed Mo_2C were anchored on N, P-codoped graphene (Mo_2C-N,P-rGO) by a facile method, during which phytic acid was employed as cross-linker to bridge the polyethyleneimine (PEI) modified graphene oxide (PEI-GO) and Mo ions through electrostatic adsorption and coordination bonding. Thanks to this ingenious strategy, the aggregation of Mo_2C usually occurred at high calcination temperature was effectively suppressed. This well-defined nanohybrid exhibits excellent activity and high stability in hydrogen evolution reaction both in acidic and basic media due to the synergistic effects of the heteroatoms doped, accessible of active sites, and conductive two dimensional (2D) structure. The obtained Mo_2C-N,P-rGO only need small overpotentials of 71 and 95 mV to drive 10 mA cm^{-2} in alkaline and acidic solution, respectively. Benefiting from the protective effect of the coated carbon layers on the Mo_2C surface, no obvious degradation was detected after 20 h of operation. This facile strategy may provide opportunities for the precisely design of functional 2D materials with unique properties.

Introduction

Hydrogen as a promising alternative to fossil fuels has attracted wide attention due to its renewable and clean properties.[1] Among all of the hydrogen evolution techniques, electrochemical hydrogen evolution reaction (HER) is the most economical and environmental friendly method.[2] While the large-scale hydrogen production by HER has been hampered by the high-cost of noble metal Pt, which is state-of-the-art electrocatalyst for HER.[3] Thus, the discovery of high-performance and earth-abundant element based electrocatalysts for HER is urgently needed.[4] Due to the Pt-like d-band electronic structure, molybdenum carbide (Mo_2C) has aroused great interest as substitute for Pt in HER process.[5–7] Until now, extensive efforts have been paid to improve the HER activity of Mo_2C, such as heterostructure construction,[8–10] nanostructure engineering,[11–15] and cation modulating strategy.[16–18] However, it is still a challenge to obtain well-defined nanostructure Mo_2C because the high carburization temperature leads to the inevitable aggregation and sintering of nanoparticles (NPs).[19,20]

Many kinds of carbon substrates, such as carbon nanosheets,[21–23] carbon nanotubes (CNTs),[24–26] and graphene[27–30] have been employed to increase the catalyst conductivity and accessibility of active sites simultaneously. Among all of the conductive substrates, graphene is supposed to be the most ideal matrix due to its excellent electron transfer ability, high chemical stability and flexibility.[31,32] Additionally, heteroatoms doping can tailor the spin density and charge distribution of graphene, which can increase its reactivity and enhance the compatibility between graphene and intermediates produced during electrocatalytic process.[33–36] Nevertheless, the reported procedures for graphene supported Mo_2C are either tedious or constructing Mo_2C with aggregated morphology.[27,37] It's still challenge to develop a facile and effective strategy to produce graphene-based nanohybrids with highly dispersed active sites and rich heteroatoms doping for HER.

In the present work, we proposed a novel approach to fabricate a 2D nanohybrid composing of monodispersed Mo_2C and N, P-codoped graphene (Mo_2C-N,P-rGO) as high performance electrocatalyst for HER. During the synthetic process, polyethyleneimine (PEI) was employed as both the nitrogen source and anchored joint guaranteeing the highly dispersion of Mo_2C.[38,39] Phytic acid, a renewable and abundant biomass with six phosphate groups, can be used as bridging ligand to cross-link Mo ions and graphene through the electrostatic adsorption and complexing of metal ions with organic ligands.[40,41] Moreover, phytic acid can provide phosphorus and carbon sources in the following carbonization process.[42] Mo_2C-N,P-rGO exhibits excellent catalytic performance for HER in terms of extremely low overpotential of 71 and 95 mV *vs* RHE at 10 mA cm^{-2} in basic and acidic solution, respectively. The carbon layers packaged on the surface prevent the aggregation and corrosion of Mo_2C effectively during the electrocatalysis process, which endow high stability to Mo_2C-N,P-rGO.[43] This strategy may provide an efficient approach for designing graphene-based functional materials with unique nanostructure.

Results and Discussion

[a] Y. Wang, S.-D. Zhu, Prof. M.-B. Wu
State Key Laboratory of Heavy Oil Processing, College of Chemical Engineering
China University of Petroleum
Qingdao 266580, China
E-mail: wumb@upc.edu.cn
[b] Y. Wang, N. Tsubaki
Department of Applied Chemistry, Graduate School of Engineering
University of Toyama
Gofuku 3190, Toyama 930-8555, Japan
E-mail: tsubaki@eng.u-toyama.ac.jp

Supporting information for this article is given via a link at the end of the document.

The highly dispersed Mo_2C NPs were anchored on the N,P-codoped graphene as illustrated in Scheme 1. Firstly, PEI-GO, phytic acid, and Mo ions mixed homogeneously were polymerized to composites with the help of electrostatic adsorption and coordination bonding through hydrothermal treatment. Afterwards, the pyrolysis process carbothermally reduced Mo ions to Mo_2C and induced the organic constituents to N or P doped carbon layers on reduced GO (rGO) or Mo_2C NPs surface. The Mo ions complexed in the polymer network at molecular scale guarantee the in situ generated Mo_2C NPs homogeneously dispersed on rGO during pyrolysis process.

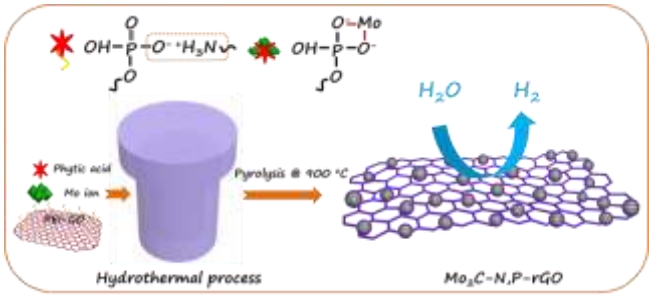

Scheme 1. Schematic of the fabrication of Mo_2C NPs anchored on N,P-codoped graphene.

The PEI modified GO provide sufficient coordination sites for anchoring Mo ions and phytic acid. Moreover, the firmly anchored precursors will prevent the aggregation of the nanoparticles during the pyrolysis process. After annealing at 900 °C, the sample maintain well 2D sheet-like structure (Figure 1a and b). Benefiting from this fantastic method, ultrafine Mo_2C NPs with narrow particle size (mean diameter 6.2 nm, Figure S1)

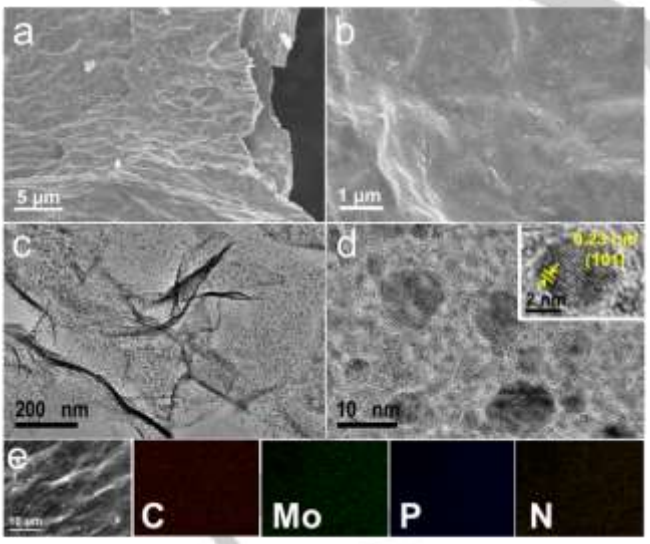

Figure 1. (a) and (b) SEM images of Mo_2C-N,P-rGO. (c) TEM and (d) HRTEM images of Mo_2C-N,P-rGO, inset is the lattice fringes corresponding to the (101) planes of Mo_2C. (e) SEM image and elemental mapping of Mo, C, P, and N of Mo_2C-N,P-rGO.

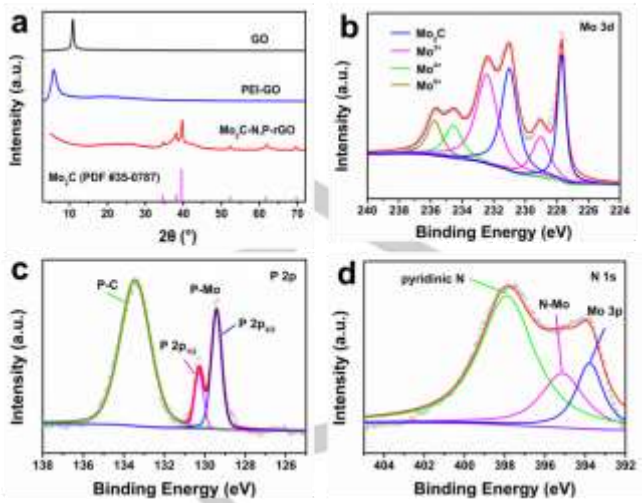

Figure 2. (a) XRD patterns of GO, PEI-GO, and Mo_2C-N,P-rGO. (b-d) High-resolution XPS spectra of (b) Mo 3d, (c) P 2p, and (d) N 1s of Mo_2C-N,P-rGO.

are homogeneously dispersed on the surface of PEI-GO as shown in Figure 1c. In the high-resolution TEM (HRTEM) image (Figure 1d and Figure S2), it's obvious that Mo_2C NPs are packaged by a few carbon layers, which can effectively prevent the aggregation and corrosion of Mo_2C NPs during electrocatalysis process. The lattice fringes with a 0.23 nm interspace corresponding to (101) lattice plane of Mo_2C can also be identified from the HRTEM image (see inset of Figure 1d). The elemental mapping of Mo_2C-N,P-rGO indicates that Mo, C, N, and P elements are distributed on the substrate homogeneously (Figure 1e).

As shown in Figure 2a, the XRD pattern of pristine GO exhibits typical peak at $2\theta = 10.9^o$, which corresponds to the 0.81 nm of d spacing. The increased interlayer space of PEI-GO (d = 1.5 nm) confirms the expansion of GO layers due to the cross-linking between PEI and GO.[44] Meanwhile, the broad peak appeared at $2\theta = 21^o$ indicates the partial reduction of GO by PEI. After hydrothermal and pyrolysis process, the characteristic peaks at 34.6, 38.0, and 39.6°, corresponding to the (100), (002), and (101) planes of hexagonal β-Mo_2C (PDF #35-0787) are observed. The diffraction peak at 26° can be attributed to the (002) diffraction peak of graphite. Additionally, no impurities are detected from the XRD pattern. Raman spectroscopy was employed to explore the variation of chemical property occurred on the surface of graphene during the synthesis process (Figure S3). Pristine GO exhibits the characteristic bands at 1350 and 1580 cm^{-1}, which are associated with the disordered carbon atoms (D band) and sp^2 hybridized graphitic carbon atoms (G band), respectively. Compared with GO (I_D/I_G = 0.80), the increased peak intensity ratio of D and G bands for PEI-GO (I_D/I_G = 0.99) indicates an increased degree of disordered structure after PEI modification. The enhanced interlayer space of PEI-GO will expose more defects, which is consistent with the results obtained from XRD spectra. The biggest intensity ratio for Mo_2C-N,P-rGO (I_D/I_G =

1.08) ascribed to the formation of large amounts of defects during the carbonization process. The electronic property of the as-prepared Mo_2C-N,P-rGO was characterized by X-ray photoelectron spectroscopy (XPS). The element content characterized by XPS is listed in Table S1. High-resolution Mo 3d XPS spectrum can be deconvoluted into six peaks, corresponding to Mo_2C (227.7 and 231.0 eV), Mo^{3+} (229.0 and 232.5 eV), Mo^{4+} (234.6 eV), and Mo^{6+} (235.8 eV) (Figure 2b). It's worth noting that the oxidative peak of Mo (Mo^{4+} and Mo^{6+}) attributed to the inevitable oxidation occurred on the surface of Mo_2C when exposed to air.[12,14] After P doping, two peaks at 129.4 and 130.3 eV assigned to P-Mo bond were formed (Figure 2c). The signal at the binding energy of 133.5 eV can be attributed to P-C bond, which illustrates the successfully doped of P species to the carbon substrate. The N 1s spectrum as shown in Figure 2d indicates that pydinic N makes predominant contribution, which has been proved to not only facilitate the electron transfer, but also act as active site for the electrocatalysis process. The typical peaks at 393.8 and 395.1 eV correspond to Mo 3p spectrum and Mo-N bond formed by carbonization treatment, respectively.

In order to better reveal the roles of PEI and phytic acid played in the synthetic process, counterpart samples were fabricated by pure GO (denote as Mo_2C-P-rGO) and without phytic acid (denote as MoO_2-N-rGO), respectively. Even though pure crystalline Mo_2C were formed in Mo_2C-P-rGO (Figure S4a), it exhibits rough morphology with Mo_2C NPs aggregated severely (Figure S4b). It's no doubt that the PEI modification is beneficial to the homogeneous dispersion of Mo_2C NPs. Only MoO_2 was detected from MoO_2-N-rGO prepared without phytic acid, which confirm that the pyrolysis of phytic acid accounts for the carburizing effect during the formation of Mo_2C (Figure S5).

Firstly, the electrocatalytic performance of Mo_2C-N,P-rGO were examined in 1 M KOH solution using a three electrode system. Mo_2C-N,P-rGO can drive a current density of 10 mA cm^{-2} at a low overpotential of 71 mV, which is higher than 30 mV obtained by the best HER catalyst Pt/C, but much less than the contrast samples Mo_2C-P-rGO and MoO_2-N-rGO (Figure 3a). The HER kinetics of Mo_2C-N,P-rGO was clarified by Tafel slope as illustrated in Figure 3b. The low Tafel slope of Mo_2C-N,P-rGO (49 mv dec^{-1}) demonstrates that it follows an electrochemical desorption controlled Volmer-Heyrovsky mechanism. In contrast, Mo_2C-P-rGO and MoO_2-N-rGO exhibit high Tafel slopes, suggesting that their HER kinetics were dominated by the Volmer step, which is a discharge process. The electrochemical impendence (EIS) were carried out to test the charge transfer efficiency of the obtained electrocatalysts. It's obvious that Mo_2C-N,P-rGO exhibits the lowest charge transfer resistence R_{CT} (48 Ω) compared with Mo_2C-P-rGO and MoO_2-N-rGO, which represents faster charge transfer (Figure 3c). The electrochemical active surface area (ECSA) were measured by calculating the double layer capacitance (C_{dl}), which is linearly proportional to the ECSA. As shown in Figure S6, the higher C_{dl} of Mo_2C-N,P-rGO (17.7 mF cm^{-2}) compared with Mo_2C-P-rGO (6.2 mF cm^{-2}) can be attributed to its much more exposed active sites. In order to clarify the structure-performance relationship of the electrocatalysts, we normalized the current density of Mo_2C-N,P-rGO and Mo_2C-P-rGO by their corresponding relative ECSA (Figure S7). The catalytic activity gap between Mo_2C-N,P-rGO and Mo_2C-P-rGO after ECSA normalization is not as obvious as that after geometric area normalization, highlighting the role of ECSA in enhancing electrocatalytic performance.[45] The much more exposed active sites thanks to the ingenious strategy endow Mo_2C-N,P-rGO with excellent HER performance. As a vital factor in practical application, long-term stability of Mo_2C-N,P-rGO was measured at a constant overpotential of 80 mV. As observed, 88.6% of current density was maintained after a long-term stability test in 1 M KOH (Figure 3d). After long-term stability test in 1 M KOH over 20 h, SEM and TEM analyses were carried to check the morphology and structure changes of Mo_2C-N,P-rGO. As shown in Figure S8, the 2D sheet-like structure was well maintained after long-term stability test. What's more, the nano-sized Mo_2C NPs were homogeneously anchored on the graphene after 20 h HER test. The carbon layers encapsulated on the surface of Mo_2C NPs effectively avoid their aggregation during HER process.

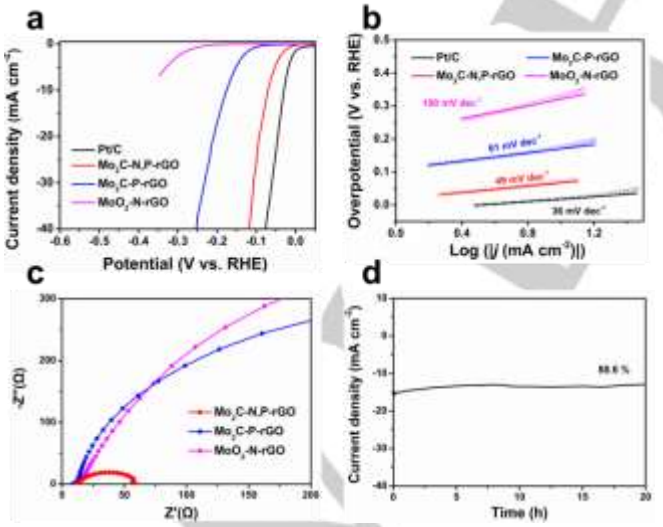

Figure 3. (a) Polarization curves of Mo_2C-N,P-rGO, Mo_2C-P-rGO, MoO_2-N-rGO, and reference Pt/C measured in 1 M KOH with a sweep rate of 5 mV s^{-1}. (b) Tafel plots of the corresponding samples in 1 M KOH. (c) Nyquist plots measured over the frequency range of 100 MHz to 0.1 Hz at an overpotential of 200 mV in 1 M KOH. (d) Long-term stability of Mo_2C-N,P-rGO at a constant overpotential of 80 mV over 20 h.

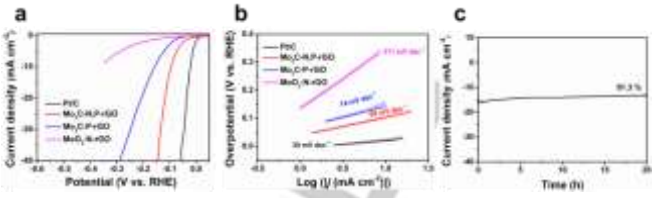

Figure 4. (a) Polarization curves and (b) Tafel plots of Mo_2C-N,P-rGO, Mo_2C-P-rGO, MoO_2-N-rGO, and reference Pt/C measured in 0.5 M H_2SO_4 with a sweep rate of 5 mV s^{-1}. (c) Long-term stability of Mo_2C-N,P-rGO at a constant overpotential of 105 mV over 20 h in 0.5 M H_2SO_4.

As we know, the metal-free carbon based electrocatalyst, especially heteroatom-doped carbon materials have been widely used in HER process. We also investigated the catalytic performance of N,P-rGO prepared by the similar method as Mo_2C-N,P-rGO except that without adding Mo sources. However, N,P-rGO exhibits poor HER activity compared with Mo_2C-N,P-rGO (Figure S9), which confirms that the activity mainly derived from the homogeneously anchored Mo_2C NPs. The graphene substrate is also indispensable for the preparation of monodispersed Mo_2C NPs. N,P-codeped Mo_2C (N,P-Mo_2C) was prepared by hydrothermal treatment of the mixture of Mo sources, phytic acid, and equivalent PEI and subsequent pyrolysis process. The obtained materials N,P-Mo_2C exhibits rough morphology as shown in the TEM image (Figure S10). The less exposed active sites of N,P-Mo_2C compared with Mo_2C-N,P-rGO lead to the poor HER activity (Figure S9).

Mo_2C-N,P-rGO also exhibits high electrocatalytic performance in acidic solution (0.5 M H_2SO_4) with low overpotential of 95 mV to achieve 10 mA cm^{-2} (Figure 4a). Additionally, the smaller Tafel slope of Mo_2C-N,P-rGO (60 mv dec^{-1}) compared with those of Mo_2C-P-rGO (74 mv dec^{-1}) and MoO_2-N-rGO (211 mv dec^{-1}) indicates its favorable HER kinetics in acidic media (Figure 4b). The chronoamperometric measurements of Mo_2C-N,P-rGO in acidic solution demonstrates that constant voltage of 105 mV can drive a stable current density with 91.3% of current density maintained even after a long-term stability test (Figure 4c). The high electrocatalytic activity and excellent stability of Mo_2C-N,P-rGO both in basic and acidic solution are comparable to other non-noble electrocatalysts reported recently (Table S2). The high electrocatalytic performance of Mo_2C-N,P-rGO can be attributed to the following points, a) highly dispersed Mo_2C anchored on the 2D graphene without aggregation, b) heteroatoms (N, P) embedded in the carbon matrix effectively modify the electro property of the catalysts, c) the packaged carbon layers on Mo_2C surface, not only prevent the aggregation of the nanoparticles, but also increase the electron transfer ability of the catalysts. Overall, synergetic effects from the advantages mentioned above boost the electrocatalytic performance of Mo_2C-N,P-rGO.

Conclusions

In summary, we constructed a graphene-based nanohybrid with uniformly dispersed Mo_2C NPs using PEI and phytic acid as crosslinker. The rGO with rich N and P contents acts as a conductive backbone to facilitate charge transfer. The highly dispersed Mo_2C NPs can increase the accessibility of the active sites. Moreover, the coated carbon layers will effectively prevent the aggregation and corrosion of Mo_2C NPs during HER process. Benefit from the unique nanostructure, Mo_2C-N,P-rGO exhibits excellent HER activity with high stability. This facile strategy may enrich the horizon of rational design of 2D functional materials for versatile applications including energy storage and catalysis.

Experimental Section

Material synthesis

Graphene oxide (GO) was prepared via modified Hummers' method. Polyethyleneimine (PEI, Sinopharm Chemical Reagent Co., Ltd.) modification was performed at 60 °C with 120 mg GO dispersed into 100 mL of 80 mg mL^{-1} PEI aqueous solution. After magnetic stirring for 12 h, PEI-GO was collected by centrifugation, repetitively washed by water, and lyophilized. Mo_2C-N,P-rGO was prepared by a facile two-step method composed of hydrothermal and calcination processes. Typically, 40 mg of PEI-GO was dispersed into 50 mL of deionized water by sonication for 2 h. Then 175 mg of ammonium molybdate tetrahydrate ($(NH_4)_6Mo_7O_{24}\cdot 4H_2O$, Sinopharm Chemical Reagent Co., Ltd.) and 940 mg of phytic acid ($C_6H_{18}O_{24}P_6$, 70%, Sinopharm Chemical Reagent Co., Ltd.) were added to the above PEI-GO solution, followed by magnetic stirring for 6 h. The obtained suspension was transferred into a 80 mL Teflon-sealed autoclave and maintained at 180 °C for 8 h. After cooling down to room temperature, the resultant product was washed with deionized water and lyophilized. Finally, Mo_2C-N,P-rGO was obtained after calcining at 900 °C for 3 h with a heating rate of 3 °C min^{-1}. For comparison, Mo_2C-P-rGO and MoO_2-N-rGO were obtained via the similar method mentioned above except that using pure GO replace PEI-GO and without adding phytic acid, respectively. N, P-codoped graphene (N,P-rGO) was also prepared by the similar method as Mo_2C-N,P-rGO except that without adding Mo sources. N,P-codeped Mo_2C (N,P-Mo_2C) was prepared by hydrothermal treatment of the mixture of Mo sources, phytic acid, and equivalent PEI and subsequent pyrolysis process.

Characterization

Sample morphologies were characterized by scanning electron microscopy (JSM-6700F, JEOL) and transmission electron microscopy (JEM-2100UHR, JEOL). The powder XRD patterns of the samples were performed on a PANalytical X-ray diffraction meter with Cu Kα radiation. Raman spectra measurements were carried out on a Renishaw Model 2000 Raman spectrometer. X-ray photoelectron spectroscopy (XPS) data was obtained from Thermo Scientific ESCALab 250Xi with monochromatic Al Kα radiation.

Measurement of electrochemical catalytic performance

The HER performance of the obtained catalysts were tested on an electrochemical analyzer (CHI 760E, CHI instruments, Inc., Shanghai) in a three-electrode system with a silver/silver chloride (Ag/AgCl) electrode as the reference electrode and a graphite rod as the counter electrode in N_2-saturated acidic (0.5 M H_2SO_4) or basic (1 M KOH) electrolyte. The working electrode was prepared as follows, 2 mg of catalyst powder was dispersed in 1 mL of water/ethanol mixed solvent (4:1, volume ratio) containing 10 μL of 10 wt% nafion solution with the help of sonication for at least 30 min. Then 15 μL of catalyst ink was coated onto a polished glassy carbon electrode (GCE, 4 mm diameter, 0.1256 mm^2) and evaporated the solvent in air to achieve a loading of ~0.24 mg cm^{-2}. The linear sweep voltammetry curves were collected at a scan rate of 5 mV s^{-1}. The electrochemical impendence spectra (EIS) was carried out from 100 MHz to 0.1 Hz at an overpotential of 200 mV. The values of electrochemical active surface area (ECSA) were determined from the linear slope of current density *vesus* scan rate in a non-faradaic region due to the ECSA was linearly proportional to the double-layer capacitances (C_{dl}). The long-term stability was tested using chronoamperometry measurements.

Acknowledgements

This work is supported by the National Natural Science Foundation of China (Nos. 51572296, U1662113) and the Fundamental Research Funds for the Central Universities (No.15CX08005A).

Keywords: N,P-codoped graphene • molybdenum carbide • unique nanostructure • hydrogen evolution reaction • electrocatalysis

[1] J. A. Turner, *Science* **2004**, *305*, 972–974.
[2] X. Zou, Y. Zhang, *Chem. Soc. Rev.* **2015**, *44*, 5148–5180.
[3] X. L. Tian, Y. Y. Xu, W. Zhang, T. Wu, B. Y. Xia, X. Wang, *ACS Energy Lett.* **2017**, *2*, 2035–2043.
[4] Y. Zheng, Y. Jiao, M. Jaroniec, S. Z. Qiao, *Angew. Chem.* **2015**, *54*, 52–65.
[5] C. Wan, Y. N. Regmi, B. M. Leonard, *Angew. Chem.* **2014**, *53*, 6407–6410.
[6] H. Vrubel, X. Hu, *Angew. Chem.* **2012**, *51*, 12703–12706.
[7] M. Miao, J. Pan, T. He, Y. Yan, B. Y. Xia, X. Wang, *Chem. Eur. J.* **2017**, *23*, 10947–10961.
[8] W. Chen, S. Iyer, S. Iyer, K. Sasaki, C. Wang, Y. Zhu, J. T. Muckerman, E. Fujita, *Energy Environ. Sci*. **2013**, *6*, 1818–1826.
[9] P. Xiao, X. Ge, H. Wang, Z. Liu, A. Fisher, X. Wang, *Adv. Funct. Mater.* **2015**, *25*, 1520–1526.
[10] J. Zhang, X. Meng, J. Zhao, Z. Zhu, *ChemCatChem* **2014**, *6*, 2059–2064.
[11] H. Fan, Y. Zheng, A. Li, Y. Ma, Q. Huo, Z. Qiao, S. Dai, *ChemCatChem* **2018**, *10*, 1–8.
[12] Y. Huang, Q. Gong, X. Song, K. Feng, K. Nie, F. Zhao, Y. Wang, M. Zeng, J. Zhong, Y. Li, *ACS Nano* **2016**, *10*, 11337–11343.
[13] H. B. Wu, B. Y. Xia, L. Yu, X. Y. Yu, X. W. Lou, *Nat. Commun.* **2015**, *6*, 6512.
[14] Y. Chen, Y. Zhang, W. Jiang, X. Zhang, Z. Dai, L. Wan, J. Hu, *ACS Nano* **2016**, *10*, 8851–8860.
[15] F. Ma, H. B. Wu, B. Y. Xia, C. Xu, X. W. Lou, *Angew. Chem.* **2015**, *54*, 15395–15399.
[16] X. Xu, F. Nosheen, X. Wang, Chem. Mater. 2016, 28, 6313–6320.
[17] C. Wan, B. M. Leonard, *Chem. Mater.* **2015**, *27*, 4281–4288.
[18] H. Lin, N. Liu, Z. Shi, Y. Guo, Y. Tang, Q. Gao, *Adv. Funct. Mater.* **2016**, *26*, 5590–5598.
[19] J. Guo, J. Wang, Z. Wu, W. Lei, J. Zhu, K. Xia, D. Wang, *J. Mater. Chem. A* **2017**, *5*, 4879–4885.
[20] Y. Zhao, K. Kamiya, K. Hashimoto, S. Nakanishi, *J. Am. Chem. Soc.* **2015**, *137*, 110–113.
[21] R. Ma, Y. Zhou, Y. Chen, P. Li, Q. Liu, J. Wang, *Angew. Chem.* **2015**, *54*, 14723–14727.
[22] Y. Liu, G. Yu, G. D. Li, Y. Sun, T. Asefa, W. Chen, X. Zou, *Angew. Chem.* **2015**, *54*, 10752–10757.
[23] C. Lu, D. Tranca, J. Zhang, Y. Su, X. Zhuang, F. Zhang, G. Seifert, X. Feng, *ACS Nano* **2017**, *11*, 3933–3942.
[24] G. Tian, Q. Zhang, B. Zhang, Y. Jin, J. Huang, D. Su, F. Wei, *Adv. Funct. Mater.* **2014**, *24*, 5956–5961.
[25] W. Chen, C. Wang, K. Sasaki, N. Marinkovic, W. Xu, J. T. Muckerman, Y. Zhu, R. R. Adzic, *Energy Environ. Sci.* **2013**, *6*, 943–951.
[26] Q. Liu, J. Tian, W. Cui, P. Jiang, N. Cheng, A. M. Asiri, X. Sun, *Angew. Chem.* **2014**, *53*, 6710–6714.
[27] J. Li, Y. Wang, C. Liu, S. Li, Y. Wang, L. Dong, Z. Dai, Y. Li, Y. Lan, *Nat. Commun.* **2016**, *7*, 11204.
[28] X. Han, C. Yu, S. Zhou, C. Zhao, H. Huang, J. Yang, Z. Liu, J. Zhao, J. Qiu, *Adv. Energy Mater.* **2017**, *7*, 1602148.
[29] C. T. Zhao, C. Yu, S. H. Liu, J. Yang, X. M. Fan, H. W. Huang, J. Qiu, *Adv. Funct. Mater*. **2015**, *25*, 6913–6920.
[30] C. Yu, X. Han, Z. Liu, C. Zhao, H. Huang, J. Yang, Y, Niu, J. Qiu, *Carbon*, **2018**, *126*, 437–442.
[31] Y. Li, H. Wang, L. Xie, Y. Liang, G. Hong, H. Dai, *J. Am. Chem. Soc.* **2011**, *133*, 7296–7299.
[32] C. Tang, H. Wang, H. Wang, Q. Zhang, G. Tian, J. Nie, F. Wei, *Adv. Mater.* **2015**, *27*, 4516–4522.
[33] H. Ang, H. T. Tan, Z. M. Luo, Y. Zhang, Y. Y. Guo, G. Guo, H. Zhang, Q. Yan, *Small* **2015**, *11*, 6278–6284.
[34] Y. Zheng, Y. Jiao, Y. Zhu, L. H. Li, Y. Han, Y. Chen, A. Du, M. Jaroniec, S. Z. Qiao, *Nat. Commun*. **2014**, *5*, 3783.
[35] J. Liang, Y. Jiao, M. Jaroniec, S. Z. Qiao, *Angew. Chem.* **2012**, *51*, 11496–11500.
[36] S. Liu, Y. Dong, C. Zhao, Z. Zhao, C. Yu, Z. Wang, J. Qiu, *Nano Energy* **2015**, *12*, 578–587.
[37] L. Pan, Y. Li, S. Yang, P. Liu, M. Yu, H. Yang, *Chem. Commun.* **2014**, *50*, 13135–13137.
[38] D. Yu, L. Dai, *J. Phys. Chem. Lett.* **2010**, *1*, 467–470.
[39] H. Yan, C. Tian, L. Sun, B. Wang, L. Wang, J. Yin, A. Wu, H. Fu, *Energy Environ. Sci.* **2014**, *7*, 1939–1949.
[40] J. Zhang, Z. Zhao, Z. Xia, L. Dai, *Nat. Nanotechnol.* **2015**, 10, 444–452.
[41] L. Pan, G. Yu, D. Zhai, H. Lee, W. Zhao, N. Liu, H. Wang, C. K. Tee, Y. Shi, Y. Cui, Z. Bao, *Proc. Natl. Acad. Sci. U. S. A.* **2012**, *109*, 9287–9292.
[42] Z. Shi, K. Nie, Z. Shao, B. Gao, H. Lin, H. Zhang, B. Liu, Y. Wang, Y. Zhang, X. Sun, X. Cao, P. Hu, Q. Gao, Y. Tang, *Energy Environ. Sci.* **2017**, *10*, 1262–1271.
[43] H. Zhang, Z. Ma, J. Duan, H. Liu, G. Liu, T. Wang, K. Chang, M. Li, L. Shi, X. Meng, K. Wu, J. Ye, *ACS Nano* **2016**, *10*, 684–694.
[44] W. Wan, L. Li, Z. Zhao, H. Hu, X. Hao, D. A. Winkler, L. Xi, T. C. Hughes, J. Qiu, *Adv. Funct. Mater*. **2014**, *24*, 4915–4921.
[45] J. Zhang, Y. Hu, D. Liu, Y. Yu, B. Zhang, *Adv. Sci.* **2017**, *4*, 1600343.

Entry for the Table of Contents

FULL PAPER

Mo_2C anchored on N,P-codoped graphene for hydrogen evolution reaction: Uniformly dispersed Mo_2C were anchored on N,P-codoped graphene (Mo_2C-N,P-rGO) by a facile method, during which phytic acid was employed as cross-linker to bridge the polyethyleneimine (PEI) modified graphene oxide (PEI-GO) and Mo ions through electrostatic adsorption and coordination bonding.

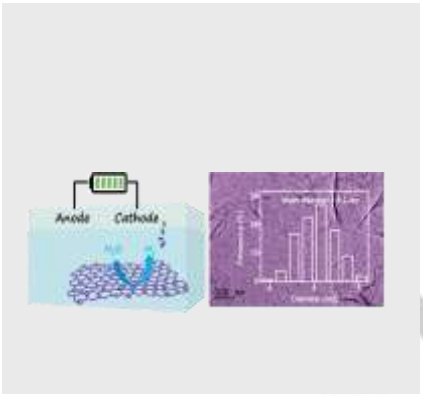

Yang Wang, Shengdong Zhu, Noritatsu Tsubaki, Mingbo Wu**

Page No. – Page No.

Highly Dispersed Mo_2C Anchored on N,P-codoped Graphene as Efficient Electrocatalyst for Hydrogen Evolution Reaction